ADVANCED SUSTAINABLE SYSTEMS
www.advsustainsys.com

Boosting the Ni-Catalyzed Hydrodeoxygenation (HDO) of Anisole Using Scrap Catalytic Converters

Alessio Zuliani, Oleg Kikhtyanin, Camilla Maria Cova, Daily Rodriguez-Padron, David Kubička, and Rafael Luque*

The large availability and renewable nature of lignin makes its upgrading to bioproducts of particular interest for sustainable development. The hydrodeoxygenation (HDO) of anisole specifically represents a model reaction for the conversion of lignin to biofuels through the removal of the aromatic carbon-oxygen bonds. To date, a range of Ni-based catalysts have been reported as highly active systems for the HDO of anisole. However, there has been a substantial lack of consideration given to the environmental characteristics of these catalytic systems, in contrast with the scope of the sustainable production of biofuels. Herein, Ni-based SiO_2 catalysts are prepared by a solventless and highly efficient mechanochemistry approach, having a considerably lower environmental impact as compared to standard impregnation methods. Importantly, scrap catalytic converters (SCATs) are employed as co-catalysts, proving the possibility of enhancing the catalytic HDO of anisole, with a scarcely exploited waste material. The results demonstrate that the combined use of Ni/SiO_2 as catalysts and Ni/SCATs as co-catalysts remarkably boosts the rate of the conversion of anisole up to more than 50% by achieving an almost complete conversion of anisole in only 40 min instead of at 200 °C and 4 MPa H_2.

1. Introduction

The societal changes and the improvement of life of the last decades have generated significant growth in the energy demand for transportation.[1] Without taking into account 2020 and 2021, remarkably influenced by COVID-19, such demand is expected to increase even more in the coming years.[2] Despite most of the national and international environmental policies, such as the UN's sustainable development goals (SDGs), are pushing for a shift in the use of alternative means of transport, i.e., electric or hydrogen vehicles,[3–5] the complete substitution of fuel-based systems will take considerable time to be completed. Indeed, the sustainable, efficient, and large-scale production of electricity or hydrogen is still not fully developed, although remarkable results are daily obtained, such as in the case of fusion energy.[6–10]

As a result, more immediate ways to reduce the excessive exploitation of fossil fuels and the consequent uncontrolled atmospheric accumulation of CO_2 are necessary.[11–14]

Currently, biofuels represent the greenest alternative to petroleum derivatives, since their use does not imply the release of fossil-stored carbon dioxide.[15] Thus, the use of biofuels for transportation can directly reduce global greenhouse gas emissions, contributing to addressing the SDG 13 "climate action."

Biofuels can be virtually produced from any renewable resource but their production from waste biomass is of particular interest. For example, biofuels produced from lignin, the second most abundant component in plant biomass, have tremendous potentialities for the sustainable production of energy, in accordance with the SDG 7, "ensure access to affordable, reliable, sustainable and modern energy for all."[16]

Nevertheless, the catalytic transformation of lignin into liquid biofuels is highly challenging, thus calling for the development of pioneering solutions.[16,17] Indeed, lignin has an extremely variable polymeric solid nature, and its structure is characterized by the abundance of carbon-oxygen bonds having low heating capacities.

Aiming at enhancing the overall calorific power of lignin through the removal of these groups, the catalytic hydrodeoxygenation (HDO) of anisole has been proposed as a model reaction

A. Zuliani, C. M. Cova, D. Rodriguez-Padron, R. Luque
Departamento de Quımica Organica
Universidad de Cordoba
Edificio Marie-Curie (C-3), Ctra Nnal IV-A, Km 396, Cordoba, Spain
E-mail: zuliani@csgi.unifi.it
A. Zuliani, C. M. Cova
CSGI – Center for Colloid and Surface Science
University of Florence
Via della Lastruccia 3, Sesto Fiorentino 50019, Italy
O. Kikhtyanin, D. Kubička
Technopark Kralupy
University of Chemistry and Technology Prague
n áměstí G. Karse 7, Kralupy nad Vltavou 278 01, Czech Republic
R. Luque
Peoples Friendship University of Russia (RUDN University)
6 Miklukho Maklaya str., Moscow 117198, Russia

The ORCID identification number(s) for the author(s) of this article can be found under https://doi.org/10.1002/adsu.202100394.

DOI: 10.1002/adsu.202100394

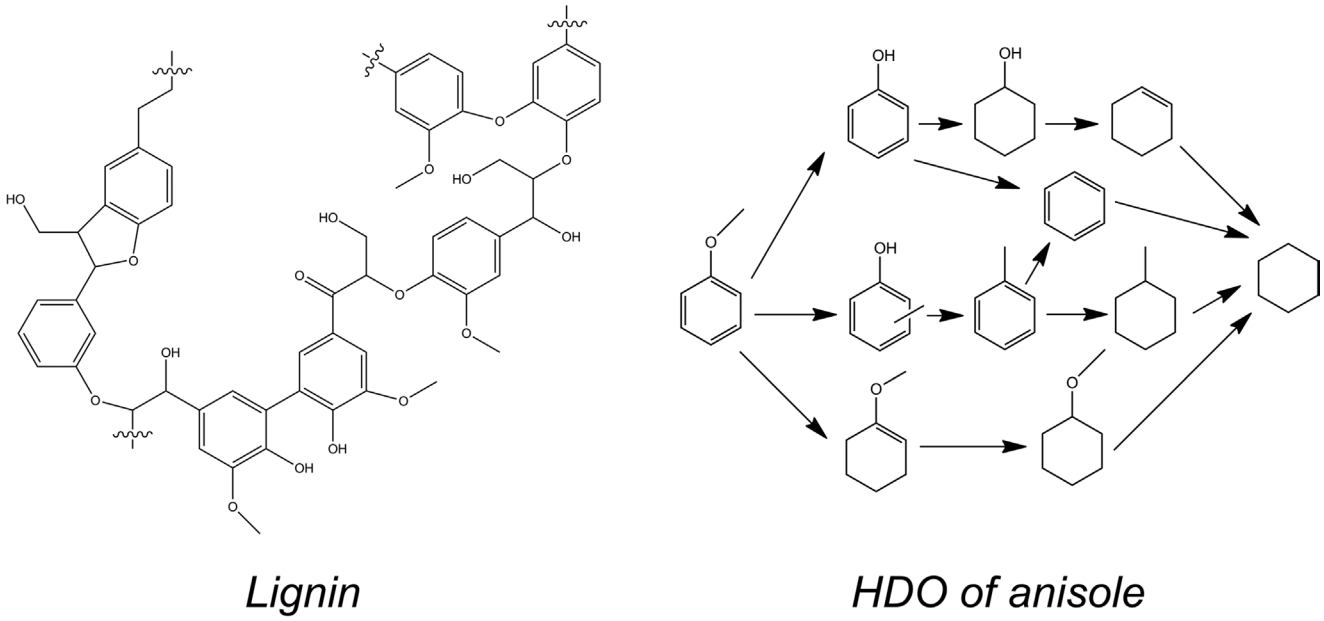

Figure 1. Representative structure of lignin and schematic paths for the hydrodeoxygenation (HDO) of anisole ideally pointing at cyclohexane, the compound with the higher heating capacity.

for the production of biofuels from the methoxy-rich compounds of lignin, as schematically illustrated in **Figure 1.**[18–21]

Among the most studied catalysts for the HDO of anisole,[22,23] nickel-based catalysts have emerged as alternative recyclable, non-precious catalysts with unique properties including high surface area, large surface energy and excellent chemical stability.[24,25] In addition, it has been proved that Ni can be potentially used for centuries if exploited in a sustainable way.[23,26] However, in contrast with the possible sustainable exploitation of this metal, most nickel-based catalysts for the HDO of anisole are produced via impregnation methods,[27,28] strongly influencing the green credentials of the synthetic process. Indeed, these synthetic approaches normally imply the disposal of large volumes of waste or the massive use of toxic reagents, in antagonism to the 12 Principles of Green Chemistry and to the concepts of SDG 13.[29,30]

More sophisticated Ni-based catalyst systems including nickel molybdenum carbides,[31] nickel phosphide, or more in general multi-metallic catalysts,[32–42] or Ni-based catalysts where the metal particles are supported on materials such as carbon nanotubes[43] or via plasma modification[44] involve the use of solvents, toxic or expensive reagents, often through long, tedious and/or energy-intense steps. Although these systems have provided remarkable advances in the field of the production of biofuels from aromatics, substantial improvements, in line with the concepts of green chemistry, are necessary to address modern environmental policies.[45,46]

Herein, Ni-based catalysts and co-catalysts for the HDO of anisole were prepared through a solventless mechanochemical approach using SiO_2 (Ni/SiO_2) and the ceramic cores of catalytic converters (Ni/SCATs) as supporting materials. The mechanochemical approach allowed the preparation of the catalysts via a solvent-free, simple, and highly reproducible procedure,[47] while the valorization of SCATs fully addressed the reusability of a largely produced waste. Indeed, more than 6 million end-of-life gasoline/diesel vehicles are yearly registered on average only in the European Union, and the resulting SCATs are generally treated by recovering only their precious metal content (i.e., platinum group metals, PGMs) via toxic and low-efficient procedures, generating large scraps of unwanted ceramic cores, also disposing of all the unrecovered metals including CeO_2 or ZrO_2.[48,49] Alternatively, the reuse of SCATS as supporting material or directly as catalysts, due to their remarkable thermal and chemical stabilities, reduce the environmental impact for the treatment of such waste,[50–52] in line with the "reduce, recycle and recovery" rules of waste management.[53]

The novel mechanochemically-prepared catalytic and co-catalytic systems including Ni/SiO_2, pure SCATs and Ni/SCATs were fully characterized by XRD, SEM, TEM and nitrogen physisorption measurements and tested in the HDO of anisole. Under commonly employed batch conditions, i.e., 200 °C and 4 MPa of H_2,[21,54] the joint use of Ni/SiO_2 and Ni/SCATs, boosted the conversion of anisole to more than 97% in only 40 min, with a rate of reaction >50% faster than the reaction catalyzed by the mere Ni/SiO_2 and by the Ni-based catalysts currently reported in the literature.

2. Results and Discussion

2.1. Characterization

In order to prepare the catalysts, SCATs were initially washed to extract and remove the carbonaceous contaminants using an ultrasonic (US) bath, among the less time consuming and energy intensive techniques for these types of purposes.[55] Thus, Ni/SiO_2 and Ni/SCATs were prepared via a solventless mechanochemical approach by first grinding together SiO_2 or washed SCATs and a Ni salt (nickel nitrate or nickel chloride) in a ball milling. In order to make it usable as co-catalysts, also

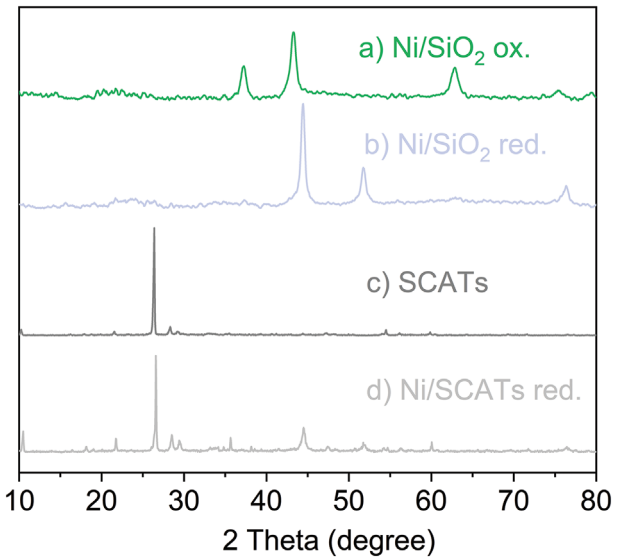

Figure 2. XRD patterns of samples: Ni/SiO_2 a) after oxidation and b) reduction step; c) scrap catalytic converters (SCATs) after the grinding procedure and d) Ni/SCATs after reduction process.

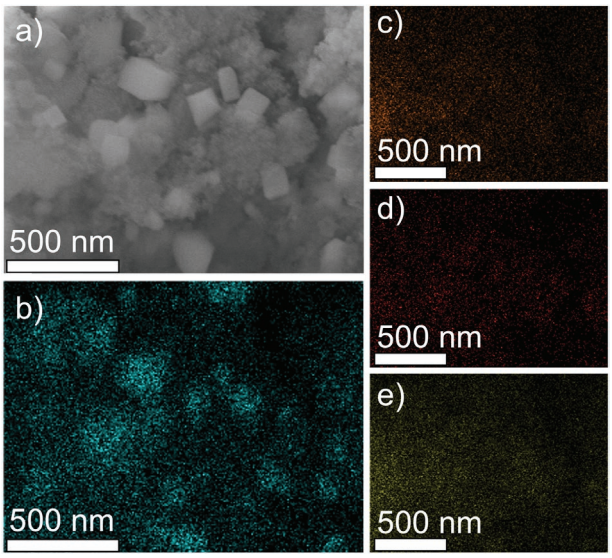

Figure 3. a) SEM image of Ni/SCATs with mapping analysis of b) Ni; c) Si; d) C; e) Al.

pure SCATs were prepared by first treating washed SCATs in a ball milling to smash the larger pieces without introducing any additional metal salt. All the grinded powders were sequentially thermally oxidized and then reduced under an H_2 atmosphere. As a comparison, the same powders were also directly reduced without performing the preliminary oxidation step.

Figure 2 shows the different XRD patterns of selected powders (see Figure S1, Supporting Information, for additional XRD patterns) prepared using nickel nitrate.

It was first observed that after the thermal oxidation treatment (Figure 2a), Ni/SiO_2 showed the presence of NiO peaks, while after the reduction process (Figure 2b) only the peaks of metallic nickel were observed. Specifically, the most intense peaks at 2θ values of 37.13°, 43.22°, 62.83°, 75.53°, and 79.51° were assigned to the (1 0 1), (0 1 2), (1 1 0), (1 1 3), and (2 0 2) planes of NiO with rhombohedral structure (JCPDS 00-044-1159), while the most intense peaks at 2θ values of 44.46°, 51.84° and 76.44° were assigned to the (1 1 1), (2 0 0) and (2 2 0) planes of metallic Ni with cubic structure (JCPDS 00-004-0850).

The XRD of washed and grinded SCATs (**Figure 3**c) showed a complex pattern composed of the diffraction peaks of the various elements of SCATs. Indeed, SCATs are normally composed of four structures: the ceramic honeycomb core (normally composed of cordierite); the wash coat, used to disperse the catalytic materials over large surface area (made of alumina, silica, titania or a mixture of them); cerium oxide or zirconium oxide coating, used to promote the storage of oxygen adsorbed from air and finally the precious metals (Pt, Rh, Pd) and additional elements such as Ni, F, and Mg.[50] Among all diffraction peaks, the most intense ones observed at 2θ values of 21.62°, 28.59° and 54.61° were indexed to the (1 0 0), (1 0 1), and (2 0 2) planes of SiO_2 with a hexagonal structure (JCPDS 00-033-1161), one of the main constituents of SCATs. Less intense diffraction peaks could be hardly assigned due to the complexity of the matrix, thus additional elemental analysis was necessary to elucidate the presence of other elements. SCATs resulted composed of Al, Si, Mg, Fe with some other minor constituents including Zn, Zr and Pt (additional details of ICP-MS analysis are reported in Table S2, Supporting Information). MP-AES quantitative analysis determined the presence of $0.7\%_{wt}$ Fe, $3\%_{wt}$ Ce and $0.1\%_{wt}$ Pt.

When Ni was supported on the SCATs (Figure 3d), forming Ni/SCATs, and the powder was reduced, the diffraction peaks of metallic nickel were clearly observable, exactly as in Ni/SiO_2 (Figure 3b).

Unsurprisingly, the use of both nickel chloride or nickel nitrate as metal precursors as well as the direct reduction of the powders without performing any preliminary oxidation process did not induce relevant changes in the XRD patterns of the resulting Ni/SiO_2, Ni/SCATs and SCATs materials (see Figure S1, Supporting Information).

According to the Debye-Scherrer's Equation,[56,57] Ni/SiO_2 after reduction treatment showed the presence of metallic Ni nanoparticles particles of ≈55 nm diameter (based on the peak at 44.4° 2θ). The XRD patterns of Ni/SCATs after the reduction step also indicated the presence of metallic Ni nanoparticles of similar dimensions. Considering the important limits of the Debye-Scherrer's equation, SEM and TEM images of sample Ni/SCATs were subsequently recorded to better investigate the morphology of the catalysts.

Figure 3 shows the SEM images and SEM mapping of Ni/SCATs. Smashed SCATs exhibited a macroscopic flake-like morphology derived from the broken honeycomb structure of SCATs. Figure 3c,d and e show the EDX-mapping of Si, C, and Al, i.e., the major components of the ceramic part. Ni (Figure 3b) was found to be in the form of crystals of 50–150 nm homogeneously distributed over the surface of SCATs (see Figure S3, Supporting Information, for SEM images with EDX mapping).

Additional TEM images of Ni/SCATs (**Figure 4**, and images Figure S4, Supporting Information) demonstrated the successful supporting of nickel nanoparticles over the scrap catalytic converter support. Some of the particles were observed in agglomerated form.

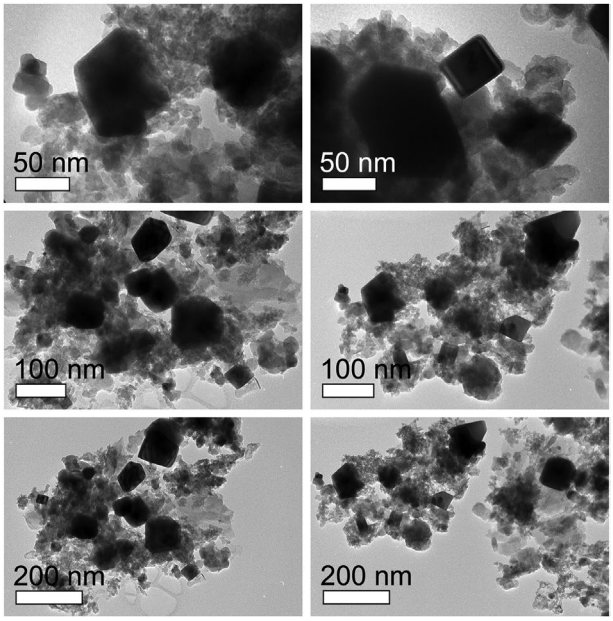

Figure 4. TEM image of Ni/SCATs.

BET (Brunauer-Emmet-Teller) physisorption analysis was carried out by nitrogen adsorption-desorption measurements. Prior to the addition of Ni, SCATs showed a surface area of ≈12 m^2 g^{-1}, close to that observed upon Ni incorporation via mechanochemistry (15 m^2 g^{-1}). After the reduction step, the surface area slightly increased (up to 20 m^2 g^{-1}), as a consequence of the reduction of the dimension of the supported metal nanoparticles. Similarly, Ni/SiO_2 showed a surface area of ≈165 m^2 g^{-1}, slightly higher than the surface area of pure SiO_2 (≈160 m^2 g^{-1}) which increased up to 180 m^2 g^{-1} after the reduction step.

The thermal stability of Ni/SiO_2 and Ni/SCATs and SCATs was subsequently studied by thermogravimetric analysis (TGA), as shown in **Figure 5**. After stabilizing the catalysts at 150 °C in order to remove adsorbed moisture, no relevant weight losses (less than 2%) were observed up to 500 °C, demonstrating the good thermal stability of the two catalysts.

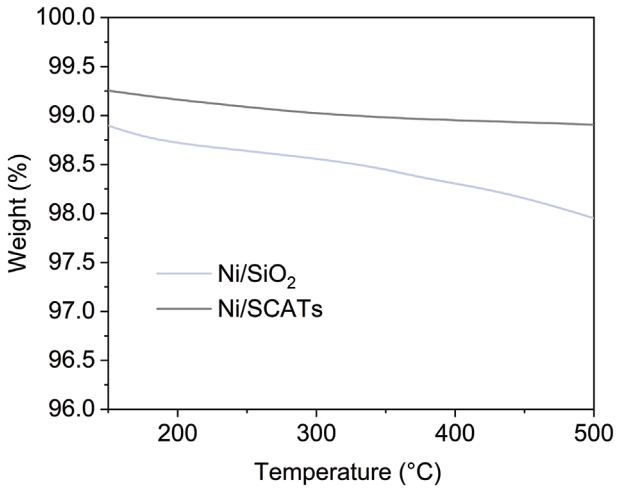

Figure 5. Thermogravimetric analysis (TGA) of Ni/SCATs and Ni/SiO_2.

2.2. Catalytic Activity

2.2.1. Influence of Ni-Catalyst Preparation

The hydrodeoxygenation (HDO) of anisole was performed in a stainless steel high-pressure and high-temperature batch reactor. The reaction was conducted operating in *n*-decane at 200 °C and 4 MPa, according to common protocols, using 100 mg of catalysts (15%$_{wt}$ of Ni).[21]

Preliminary experiments were carried out aiming to explore the catalytic performances of Ni/SiO_2 produced via mechanochemical approach as compared to the Ni/SiO_2 prepared through a standard impregnation method (Ni/SiO_2 impregnation), as shown in **Figure 6**.

In the studied reaction conditions, Ni/SiO_2 catalyst prepared via impregnation method exhibited a sensibly lower catalytic activity to that of mechanochemical Ni/SiO_2, proving the efficiency of the mechanochemical method for the preparation of active catalysts. It must be highlighted that sample "Ni/SiO_2 impregnation" was prepared through the easiest possible impregnation method, without considering elaborated procedures such as those for the preparation of Ni nanoparticles., which are specifically aimed at enhancing the efficiency of the Ni-based catalysts but are too complicated to be compared with the smooth mechanochemical approach.

The selectivity to the different products highlighted the possible reaction path: 1-methoxycyclohexane (>90%) was found to be the major product, followed by 1,1'-oxybis(cyclohexane), cyclohexane and benzene, indicating that the hydrogenation of the aromatic ring was favored to the cleavage of the ether group (Figure 1). The results were in good accordance with the literature, and the operative conditions were thus selected as indicative to prove the potentialities of Ni-base catalysts for the HDO.

ICP-MS analysis of the solution after reaction did not reveal the presence of Ni, proving the good stability of the catalyst. Grinding of the metal salt together with SiO_2 followed by reduction allowed embedding and stabilizing Ni nanoparticles over the supporting material without detectable losses, offering a

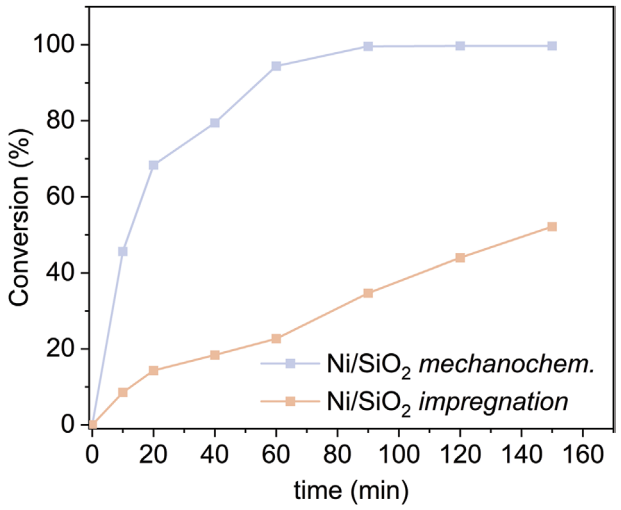

Figure 6. Conversion values of the hydrodeoxygenation (HDO) of anisole catalyzed by mechanochemically prepared Ni/SiO_2 at 200 °C and 4 MPa H_2.

Table 1. Comparison of selected characteristics for mechanochemical versus incipient impregnation methods for the preparation of Ni/SiO_2 catalysts.

Preparation approach	Toxic reagents/solutions	Preparation steps	E-factor
Mechanochemical	Ni salt	Grinding; thermal treatment	0.1–0.3
Incipient impregnation	Ni salt; water solution of the salt	Impregnation; evaporation; thermal treatment	>30

valid alternative to Ni incorporation through dissolution and precipitation of the metal salt (as in the impregnation method). The prepared catalysts were further studied concerning green characteristics. In detail, as shown in **Table 1**, the sustainable properties of the two preparation methods were analyzed in terms of the use of toxic reagents and solvents, simplicity of preparation (i.e., number of steps involved in the different procedures), and the environmental factor (E-factor),[30] calculated as the ratio of the mass of waste generated per mass of the product (i.e., catalyst).

Nickel salt was the only toxic reagent employed in the mechanochemical (solid state/solventless) method, while the incipient impregnation approach also involved the dissolution of the Ni salt in water, implying the use of additional reagents. Second, the mechanochemical approach was carried out in two steps, i.e., grinding of metal salt with SiO_2 and sequential thermal treatment (eventually with direct reduction of Ni under molecular hydrogen), while the impregnation method involved the impregnation of the catalyst with the metal salt followed by evaporation of the solution and thermal treatment (also in this case eventually with direct reduction of Ni under molecular hydrogen). This latter approach was thus more energy and time consuming than the mechanochemical method. Finally, and more importantly, the environmental factor (E-factor), one of the most employed metrics for the determination of waste produced in a process, was also calculated. The E-factor of the mechanochemical approach was remarkably reduced as compared to that of the impregnation method. Indeed, the waste produced by the mechanochemical approach only derived from the water used for the cleaning of the milling jar (≈0.1–0.2 kg of water per kg of product), while the impregnation method, besides water and solvents used for cleaning various tools, also involved the massive use of an aqueous solution for the dissolution of the Ni salt. These results demonstrated that the mechanochemical approach had more environmentally friendly characteristics to prepare catalytically active Ni/SiO_2 materials with respect to the standardly employed incipient impregnation method. In addition, mechanochemistry has been pointed as a promising tool for a sustainable development due to its important scale-up properties,[58–61] key features for the making of a catalyst for biofuel production from aromatics.[62–64]

2.2.2. Influence of the Reduction In Situ of Ni/SiO_2

The catalytic activity of Ni/SiO_2 was subsequently studied by comparing the activity of Ni/SiO_2 reduced and stored before the reaction with the activity of Ni/SiO_2 reduced in situ, as shown in **Figure 7**.

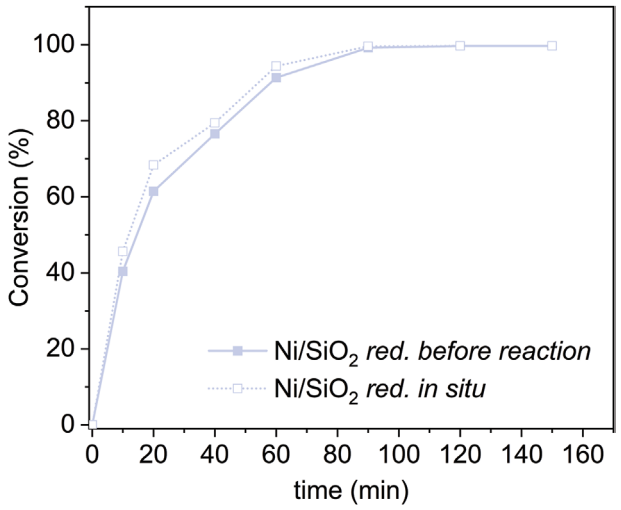

Figure 7. Conversion values of the hydrodeoxygenation (HDO) of anisole catalyzed by Ni/SiO_2 reduced before reaction and in situ (200 °C, 4 MPa H_2, 100 mg of catalyst).

Results indicated that the reduction of the catalysts could have some influence on the reaction kinetics. However, the rate of reaction was slightly improved when using in situ reduced catalysts, demonstrating the good stability of the catalyst reduced and stored before the reaction, with important advantages for scaling up design (the use of already reduced catalysts remarkably decrease the total time of the process). The reason for this marginally enhanced activity can be explained as possible partial oxidation of previously reduced catalyst (the reduction potential of Ni^{2+} is only –0.25 V, but truly not detectable in XRD analysis) or more likely as a consequence of hydrogen adsorption on the in situ reduced catalyst.

2.2.3. Influence of the Use of Different Ni Salts

The use of different Ni salts for the preparation of Ni/SiO_2 catalysts was thus explored by preparing Ni-catalysts using $NiCl_2$ precursor as an alternative to $Ni(NO_3)_2 \cdot 6H_20$, considering that the formation of $NiCl_2$ (using HCl) is one of the most efficient ways to recover nickel from Ni-enriched waste, such as spent metal batteries.[65] As expected by XRD analysis previously described (Section 2.1), no relevant variation in catalytic activities of the catalysts was noticed (both showing >98% of conversion of anisole in 90 min with the same selectivity to products), proving the possibility of using waste-recovered $NiCl_2$ (see Figure S5, Supporting Information).

2.2.4. Influence of Employing SCATs as Co-Catalyst

The use of SCATs as co-catalyst was thus explored by carrying out the reaction in the presence of a physical mixture of Ni/SiO_2 and SCATs (100 mg of $15\%_{wt}Ni/SiO_2$ and 50 mg of SCATs), as illustrated in **Figure 8**.

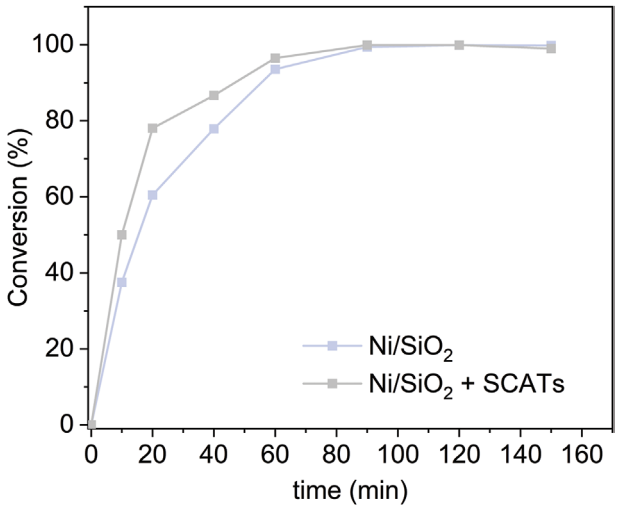

Figure 8. Conversion values of the hydrodeoxygenation (HDO) of anisole catalyzed by Ni/SiO_2 and scrap catalytic converters (SCATs) (200 °C, 4 MPa H_2, 100 mg of Ni/SiO_2 and 50 mg of SCATs)).

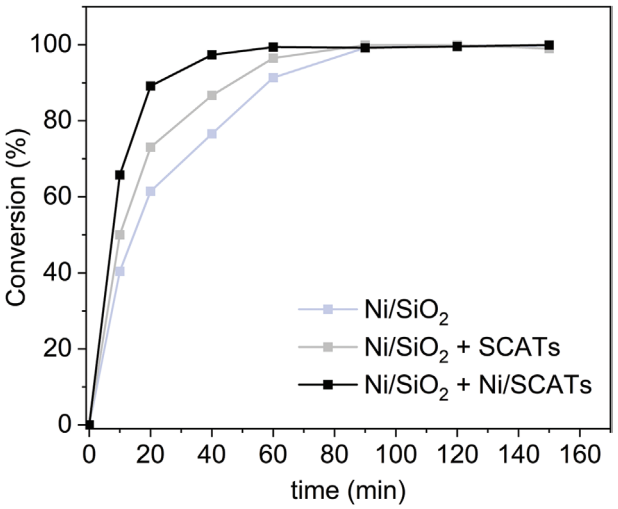

Figure 9. Conversion values of the hydrodeoxygenation (HDO) of anisole catalyzed by Ni/SiO_2 (100 mg), Ni/SiO_2+SCATs (100 mg and 50 mg respectively) and $NiSiO_2$+Ni/SCATs (50 mg each one) at 200 °C and 4 MPa H_2.

The results demonstrated that the use of SCATs as co-catalyst could significantly improve the conversion of anisole through the HDO. Indeed, SCATs contain metals such as Pt, Ru and Pd (Section 2.1), which are, according to the literature, highly efficient in the HDO reaction. However, the use of SCATs, i.e., PMGs-enriched waste, has remarkably lower costs than the synthesis of precious metal-based catalysts, considering that SCATs are a waste widely available and cheap. Consequently, the use of SCATs as co-catalyst could boost the catalytic activity of Ni/SiO_2 without relevant additional costs to the production process, in contrast with commonly employed strategies resorting to the use of additional expensive metals. The ICP-MS analysis of the solution after reaction did not detect the presence of metals, proving the good stability of the SCATs.

2.2.5. Influence of Employing Ni/SCATs as Co-Catalyst

The activity of SCATs as co-catalyst was further investigated by supporting Ni over SCATs by a mechanochemical approach, following the same procedure as for the preparation of Ni/SiO_2. The reaction was thus carried out by mixing Ni/SiO_2 and Ni/SCATs. As shown in **Figure 9**, the presence of Ni/SiO_2 as catalysts and Ni/SCATs as co-catalyst (keeping the same total Ni content of previous experiments) remarkably boosted the rate of conversion of anisole, obtaining more than 97% conversion in only 40 min, while the same conversion was obtained only after more than 60 min of reaction employing Ni/SiO_2 (additional data related to selectivity can be found in Table S6–S8, Supporting Information).

As summarized in **Table 2**, the obtained results were superior to reported data to date in HDO using Ni-Si-based catalysts, obtaining an almost complete conversion of anisole in more than 50% less time than referential literature, significantly improving the know-how related to the HDO of anisole.

Again, the ICP-MS analysis of the solution after reaction did detect the presence of Ni, nor other metals, proving the good stability of both the Ni/SiO_2 and the Ni/SCATs catalyst and co-catalyst. Additional reusability tests proved the possible reutilization of the catalysts in the same reaction conditions for more

Table 2. Reported data of the HDO of anisole catalyzed by Ni-Si based systems in comparison with the results of this work.

Ni- catalyst	*T* [°C]	*p* [MPa]	Preparation method	Catalyst [mg]	Reactant [%wt].and solution [Ml]	Time [min]to >97% conv.	Ref.
$10\%_{wt}$ Ni/SiO_2	220	4	Impregnation	100	8, 20	90	[21]
$5\%_{wt}$ Ni/HZSM-5	200	6.8	Impregnation	300	4.5, 50	140	[27]
$10\%_{wt}$ Ni/SBA-15	280	4.8	Impregnation	100	5, 50	360	[54]
$5\%_{wt}$ Ni/USY zeolites	200	5.1	Impregnation	100	6, 50	140	[66]
$5\%_{wt}$ Ni/IM-5 zeolite	200	5	Impregnation	50	6, 24.5	140	[67]
$5\%_{wt}$ Ni/USY zeolite	200	5.1	Impregnation	100	4, 55	>150	[68]
$15\%_{wt}$ Ni/SiO_2	200	4	Mechanochemical	100	5, 70	90	This work
$15\%_{wt}$ Ni/SiO_2 + SCATs	200	4	Mechanochemical	100 + 100	5, 70	80	This work
$15\%_{wt}$ Ni/SiO_2 + $15\%_{wt}$ Ni/SCATs	200	4	Mechanochemical	50 + 50	5, 70	40	This work

than four cycles, with no detectable differences in the conversion values after reactivation of the catalysts and co-catalysts through hydrogenation, in good accordance with the literature regarding catalysts prepared with SCATs.[50–52]

3. Conclusions

An innovative and environmentally friendly catalytic system for the hydrodeoxygenation of anisole is disclosed, composed of mechanochemically synthesized Ni/SiO_2 (acting as a catalyst) and waste-derived Ni/SCATs as co-catalysts. The use of co-catalysts remarkably improved the overall anisole conversion. Results demonstrated the possibility of obtaining >97% of conversion in 40 min of reaction at 200 °C and 4 MPa H_2, boosting the rate of the reaction of more than >50%, in comparison with Ni/SiO_2 and reported data. Due to the low environmental impact of the mechanochemical approach as well as the use of waste materials, i.e., SCATs, the novel catalytic system exhibits significantly improved green credentials including reduced waste production, use of low toxic chemicals and high energy efficiency, with promising potentialities for scaled-up production and continuous flow applications. Further investigations will lead to the enhancement of various other reactions to produce biofuels from aromatics (including from lignin) exploiting the cheap and largely available scrap ceramic cores of catalytic converters.

4. Experimental Section

Materials: Anisole (99%) used as lignin model compound was purchased from Alfa Aesar. *n*-decane (≥94%) used as solvent was purchased Penta Chemicals Unlimited. n-octane (≥99%) used as an internal standard was purchased from EMO Millipore Group. $NiCl_2$, $Ni(NO_3)_2{\cdot}6H_2O$, SiO_2 (50–70 mesh particle size) were purchased from Sigma Aldrich. All reagents were used without any further purification. Scrap ceramic cores of catalytic converters (SCATs) were kindly donated by the company Provaluta S.L. (Cordoba, Spain).

Preparation of SCATs: Prior to utilization, SCATs were washed and dried to remove all the superficial carbonaceous residuals and other pollutant residues. More in detail, 50 g of SCATs were dispersed in 100 mL of distilled water and ethanol (1:1). Sequentially, the mixture was ultrasonicated in a US bath for 2 h for a sequence of washing cycles (due to US thermal effects, the temperature increased up to ≈50 °C). When no losses of weight were observed, the washing cycles were stopped. A thermal treatment was successively performed to perfectly clean the surface of the metals present in the SCATs and remove the last residuals. Specifically, the powders were heated for 1 h under N_2 flux and for 3 h under $10\%_{vol}$ H_2 flux at 500 °C in a tubular furnace. Thus, the powders were cooled down to room temperature under the nitrogen stream.

Supporting Ni: $15\%_{wt}$ Ni-supported catalysts were prepared by a mechanochemical approach. In a typical synthesis, the supporting powder (SiO_2 or eventually SCATs) and the correct amount of nickel salt ($NiCl_2$ or $Ni(NO_3)_2{\cdot}6H_2O$) were mixed in a 125 mL stainless steel milling jar equipped with eighteen 5 mm diameter stainless steel balls. The powders were grounded in a Retsch PM100 planetary ball mill at 350 rpm for 15', changing the direction of rotation every 150 s. Upon milling, the resulting homogenous powders were thermally treated. In detail, the powders were treated in a tubular furnace for 1 h under N_2 and for 4 h under N_2 and 10%vol H_2 flux at 550 °C. If the reduction was designed to be performed in situ in the reactor, the thermal treatment was carried out without hydrogen. Finally, the powders were cooled down to room temperature under N_2 flux.

Preparation of Ni/SiO_2 by Impregnation Method: SiO_2 was incipiently impregnated with an aqueous solution of Ni nitrate in order to have a final concentration of $15\%_{wt}$. The resultant powder was left at room temperature for 24 h, followed by drying at 120 °C for 12 h and calcination at 550 °C in the air for 4 h to get the catalyst precursors in the oxidation state. Second, the catalyst was heated for 1 h under N_2 flux and for 3 h under $10\%_{vol}$ H_2 flux at 550 °C.

Catalyst Characterization: Powder X-ray diffraction (XRD) patterns were obtained with a Bruker D8 DISCOVER A25 diffractometer (PanAnalytic/Philips, Lelyweg, Almelo, The Netherlands) using CuKα (λ = 1.5418 Å) radiation. Wide angle scanning patterns were collected over a 2θ range from 10° to 80° with a step size of 0.018° and counting time of 5 s per step.

Textural properties of the samples were determined by nitrogen physisorption using a Micromeritics ASAP 2020 automated system (Micromeritics Instrument Corporation, Norcross, GA, USA) using the Brunauer-Emmett-Teller (BET) method. Prior to analysis, the samples were outgassed for 24 h at 100 °C under vacuum ($P_0 = 10^{-2}$ Pa) and subsequently analysed.

Scanning electron microscopy images were recorded with a JEOL JSM-6300 scanning microscope (JEOL Ltd, Peabody, MA, USA) equipped with energy-dispersive X-ray spectroscopy (EDX) at 15 kV.

TEM images were recorded with a FEI Tecnai G2 system, equipped with a charge-coupled device (CCD) camera. Samples were previously suspended in ethanol and subsequently deposited on a copper grid.

The metallic composition of the catalysts was determined by inductively coupled plasma mass spectrometry (ICP-MS) and by Microwave Plasma Atomic Emission Spectroscopy (MP-AES) (Agilent 4100 MP-AES). The analysis was carried out by digesting 20 mg of the selected catalyst with 5 mL of nitric acid (HNO_3) and hydrochloric acid (HCl) in a volume ratio of 1 : 3 at 473 K for 20 in a microwave oven (Milestone Ethos Plus, Milestone Srl).

Hydrodeoxygenation (HDO) Reactions: The reaction of hydrodeoxygenation of anisole was carried out in a 300 mL stainless steel high-pressure and high-temperature batch reactor (equipped with a reaction controller model 4848B Parr). When necessary, prior to perform the reaction, 100 mg of the different catalysts were added to the reactor, sealed, and purged with nitrogen 15' to ensure the removal of air. The reactor was then purged with hydrogen at room temperature for 5'. Catalysts were sequentially reduced for 2 h (time recording initiated when the temperature reached the selected reduction temperature) using a heating rate of ≈12 °C min^{-1}. After reduction, the reactor was cooled in the hydrogen atmosphere to rt and sequentially purged with nitrogen for 15'. Elsewhere, catalysts were directly added to the reactant mixture.

The reactant mixture was prepared by mixing anisole, *n*-decane, and *n*-octane. After the catalyst reduction and cooling step, the reactor was opened, and the reaction mixture (70 mL *n*-decane $5\%_{wt}$ anisole using n-octane as internal standard) was quickly poured into the reactor. N_2 was then flowed through the reactor for 15' at a stirring rate of 300 rpm to ensure no residual air was present. The reactor was then purged with hydrogen for 5' and then heated up to 100 °C at 300 rpm. At 100 °C, the reactor was pressurized at 0.5 MPa H_2 pressure and heated up to final temperature. When the reactor reached the final temperature, the hydrogen pressure was increased up to final pressure (4 MPa) and the stirring rate increased up to 700 rpm. The reaction time was set to zero at this point. The reaction was monitored by withdrawing aliquots of the reaction mixture at different times. At the end of the reaction, the reactor was cooled to room temperature. The influence of the removal of aliquots of solution during the reaction was checked by performing some additional experiments specifically carried out by taking only one aliquot of solution at a selected time. No difference between the reaction with several aliquots taken and the reaction with only an aliquot was observed.

The conversion and selectivity were analyzed by gas chromatography (GC) in an Agilent 7820A gas chromatography using a flame ionization detector (FID). A capillary column, HP-5 as employed. Calibration curves were obtained with an internal standard method using *n*-octane as the

standard. Standard solutions of anisole (from 0.0156 to 0.600 M) and *n*-octane in *n*-decane were analyzed by GC to give linear regressions with $R^2 > 0.999$ (specifically, 0.99931).

Supporting Information

Supporting Information is available from the Wiley Online Library or from the author.

Acknowledgements

This work was supported by RUDN University Strategic Academic Leadership Program (R.L.).

Funding for open access charge: Universidad de Córdoba/CBUA.

Conflict of Interest

The authors declare no conflict of interest.

Data Availability Statement

The data that support the findings of this study are available in the supplementary material of this article.

Keywords

anisole, biofuels, biomass, catalytic converters, hydrodeoxygenation, lignin, nickel

Received: October 13, 2021
Revised: February 10, 2022
Published online: March 16, 2022

[1] M. H. Mousavi, S. Ghavidel, *Case Stud.* **2019**, *7*, 423.
[2] A. Rashedi, T. Khanam, M. Jonkman, *Energies* **2020**, *13*, 6048.
[3] T. Zeng, C. Z. Zhang, D. Hao, D. P. Cao, J. W. Chen, J. R. Chen, J. Li, *Energy* **2020**, *208*, 118319.
[4] J. Kurtz, T. Bradley, E. Winkler, C. Gearhart, *Int. J. Hydrogen Energy* **2020**, *45*, 32298.
[5] A. Zuliani, M. Cano, F. Calsolaro, A. R. Puente Santiago, J. J. Giner-Casares, E. Rodríguez-Castellón, G. Berlier, G. Cravotto, K. Martina, R. Luque, *Sustainable Energy Fuels* **2021**, *5*, 720.
[6] H. Moon, I. S. Chang, K. H. Kang, J. K. Jang, B. H. Kim, *Biotechnol. Lett.* **2004**, *26*, 1717.
[7] C. M. Cova, A. Zuliani, A. R. P. Santiago, A. Caballero, M. J. Munoz-Batista, R. Luque, *J. Mater. Chem. A* **2018**, *6*, 21516.
[8] M. Longhi, C. Cova, E. Pargoletti, M. Coduri, S. Santangelo, S. Patane, N. Ditaranto, N. Cioffi, A. Facibeni, M. Scavini, *Nanomaterials* **2018**, *8*, 643.
[9] M. C. Handley, D. Slesinski, S. C. Hsu, *J. Fusion Energy* **2021**, *40*, https://doi.org/10.1007/s10894-021-00306-4.
[10] E. G. Nicholas, T. P. Davis, F. Federici, J. Leland, B. S. Patel, C. Vincent, S. H. Ward, *Energy Policy* **2021**, *149*, 112043.
[11] F. Ivars-Barcelo, A. Zuliani, M. Fallah, M. Mashkour, M. Rahimnejad, R. Luque, *Appl. Sci.* **2018**, *8*, 1184.
[12] S. L. Piao, Q. Liu, A. P. Chen, I. A. Janssens, Y. S. Fu, J. H. Dai, L. L. Liu, X. Lian, M. G. Shen, X. L. Zhu, *Global Change Biol.* **2019**, *25*, 1922.
[13] A. Zuliani, C. M. Cova, *Photochem* **2021**, *1*, 147.
[14] C. M. Cova, E. Rincón, E. Espinosa, L. Serrano, A. Zuliani, *Biosensors* **2022**, *12*, 51.
[15] A. Zuliani, F. Ivars, R. Luque, *ChemCatChem* **2018**, *10*, 1968.
[16] R. S. Ma, Y. Xu, X. Zhang, *ChemSusChem* **2015**, *8*, 24.
[17] J. Lofstedt, C. Dahlstrand, A. Orebom, G. Meuzelaar, S. Sawadjoon, M. V. Galkin, P. Agback, M. Wimby, E. Corresa, Y. Mathieu, L. Sauvanaud, S. Eriksson, A. Corma, J. S. M. Samec, *ChemSusChem* **2016**, *9*, 1392.
[18] X. L. Zhu, R. G. Mallinson, D. E. Resasco, *Appl. Catal., A* **2010**, *379*, 172.
[19] L. Zhu, L. L. Lobban, R. G. Mallinson, D. E. Resasco, *J. Catal.* **2011**, *281*, 21.
[20] K. L. Li, R. J. Wang, J. X. Chen, *Energy Fuel.* **2011**, *25*, 854.
[21] S. H. Jin, Z. H. Xiao, C. Li, X. Chen, L. Wang, J. C. Xing, W. Z. Li, C. H. Liang, *Catal. Today* **2014**, *234*, 125.
[22] P. Bhongale, S. Joshi, N. Mali, *Catal. Rev.* **2021**, 1, https://doi.org/10.1080/01614940.2021.1930490.
[23] M. Saidi, F. Samimi, D. Karimipourfard, T. Nimmanwudipong, B. C. Gates, M. R. Rahimpour, *Energy Environ. Sci.* **2014**, *7*, 103.
[24] A. G. Sergeev, J. F. Hartwig, *Science* **2011**, *332*, 439.
[25] A. Zuliani, A. M. Balu, R. Luque, *ACS Sustainable Chem. Eng.* **2017**, *5*, 11584.
[26] M. Henckens, E. Worrell, *J. Cleaner Prod.* **2020**, *264*, 121460.
[27] W. L. Li, F. Li, H. Y. Wang, M. J. Liao, P. Li, J. J. Zheng, C. Y. Tu, R. F. Li, *Mol. Catal.* **2020**, *480*, 110642.
[28] P. H. Yan, E. Kennedy, M. Stockenhuber, *Green Chem.*. **2021**, *23*, 4673.
[29] P. Anastas, N. Eghbali, *Chem. Soc. Rev.* **2010**, *39*, 301.
[30] R. A. Sheldon, *Green Chem.*. **2017**, *19*, 18.
[31] A. A. Smirnov, Z. Geng, S. A. Khromova, S. G. Zavarukhin, O. A. Bulavchenko, A. A. Saraev, V. V. Kaichev, D. Y. Ermakov, V. A. Yakovlev, *J. Catal.* **2017**, *354*, 61.
[32] S. A. Khromova, A. A. Smirnov, O. A. Bulavchenko, A. A. Saraev, V. V. Kaichev, S. I. Reshetnikov, V. A. Yakovlev, *Appl. Catal., A* **2014**, *470*, 261.
[33] A. A. Smirnov, S. A. Khromova, O. A. Bulavchenko, V. V. Kaichev, A. A. Saraev, S. I. Reshetnikov, M. V. Bykova, L. I. Trusov, V. A. Yakovlev, *Kinet. Catal.* **2014**, *55*, 69.
[34] A. A. Smirnov, S. A. Khromova, D. Y. Ermakov, O. A. Bulavchenko, A. A. Saraev, P. V. Aleksandrov, V. V. Kaichev, V. A. Yakovlev, *Appl. Catal., A* **2016**, *514*, 224.
[35] S. Pichaikaran, P. Arumugam, *Green Chem.*. **2016**, *18*, 2888.
[36] S. H. Jin, W. X. Guan, C. W. Tsang, D. Y. S. Yan, C. Y. Chan, C. H. Liang, *Catal. Lett.* **2017**, *147*, 2215.
[37] X. F. Wang, J. X. Chen, *Chin. J. Catal.* **2017**, *38*, 1818.
[38] T. L. R. Hewer, A. G. F. Souza, K. T. C. Roseno, P. F. Moreira, R. Bonfim, R. M. B. Alves, M. Schmal, *Renewable Energy* **2018**, *119*, 615.
[39] Y. Zheng, N. Zhao, J. X. Chen, *Appl. Catal., B* **2019**, *250*, 280.
[40] B. Pomeroy, T. Doxtator, J. E. Herrera, D. Pjontek, *Int. J. Chem. React. Eng.* **2020**, *18*, https://doi.org/10.1515/ijcre-2019-0066.
[41] Y. J. Han, L. Ai, Y. T. Shi, J. X. Chen, *J. Energy Inst.* **2021**, *98*, 20.
[42] N. S. Nesterov, A. A. Smirnov, V. P. Pakharukova, V. A. Yakovlev, O. N. Martyanov, *Catal. Today* **2021**, *379*, 262.
[43] H. Taghvaei, A. Bakhtyari, M. R. Rahimpour, *Fuel* **2021**, *288*, 119698.
[44] H. Taghvaei, M. R. Rahimpour, P. Bruggeman, *RSC Adv.*. **2017**, *7*, 140.
[45] C. Kroll, A. Warchold, P. Pradhan, *Palgrave Commun.* **2019**, *5*, 140.
[46] L. Ohnesorge, E. Rogge, *Eur. Co. Law* **2021**, *18*, 34.
[47] S. L. James, C. J. Adams, C. Bolm, D. Braga, P. Collier, T. Friscic, F. Grepioni, K. D. M. Harris, G. Hyett, W. Jones, A. Krebs, J. Mack, L. Maini, A. G. Orpen, I. P. Parkin, W. C. Shearouse, J. W. Steed, D. C. Waddell, *Chem. Soc. Rev.* **2012**, *41*, 413.
[48] C. H. Kim, S. I. Woo, S. H. Jeon, *Ind. Eng. Chem. Res.* **2000**, *39*, 1185.

[49] H. Brandl, S. Lehmann, M. A. Faramarzi, D. Martinelli, *Hydrometallurgy* **2008**, *94*, 14.
[50] C. M. Cova, A. Zuliani, M. J. Munoz-Batista, R. Luque, *Green Chem.*. **2019**, *21*, 4712.
[51] A. Zuliani, C. M. Cova, R. Manno, V. Sebastian, A. A. Romero, R. Luque, *Green Chem.*. **2020**, *22*, 379.
[52] C. M. Cova, A. Zuliani, R. Manno, V. Sebastian, R. Luque, *Green Chem.*. **2020**, *22*, 1414.
[53] S. Sakai, H. Yoshida, Y. Hirai, M. Asari, H. Takigami, S. Takahashi, K. Tomoda, M. V. Peeler, J. Wejchert, T. Schmid-Unterseh, A. Ravazzi Douvan, R. Hathaway, L. D. Hylander, C. Fischer, G. J. Oh, L. Jinhui, N. K. Chi, *J. Mater. Cycles Waste Manage.* **2011**, *13*, 86.
[54] H. Vargas-Villagran, M. A. Flores-Villeda, I. Puente-Lee, D. A. Solis-Casados, A. Gomez-Cortes, G. Diaz-Guerrero, T. E. Klimova, *Catal. Today* **2020**, *349*, 26.
[55] C. M. Cova, L. Boffa, M. Pistocchi, S. Giorgini, R. Luque, G. Cravotto, *Molecules* **2019**, *24*, 2681.
[56] M. Arshad, M. Asghar, M. Junaid, M. F. Warsi, M. N. Rasheed, M. Hashim, M. A. Al-Maghrabi, M. A. Khan, *J. Magn. Magn. Mater.* **2019**, *474*, 98.
[57] F. Ferlin, T. Giannoni, A. Zuliani, O. Piermatti, R. Luque, L. Vaccaro, *ChemSusChem* **2019**, *12*, 3178.
[58] T. Friscic, C. Mottillo, H. M. Titi, *Angew. Chem., Int. Ed.* **2020**, *59*, 1018.
[59] K. J. Ardila-Fierro, J. G. Hernandez, *ChemSusChem* **2021**, *14*, 2145.
[60] S. Mateti, M. Mathesh, Z. Liu, T. Tao, T. Ramireddy, A. M. Glushenkov, W. R Yang, Y. I. Chen, *Chem. Commun.* **2021**, *57*, 1080.
[61] B. G. Fiss, A. J. Richard, T. Friscic, A. Moores, *Can. J. Chem.* **2021**, *99*, 93.
[62] A. Agarwal, M. Rana, J. H. Park, *Fuel Process. Technol.* **2018**, *181*, 115.
[63] Z. Wu, L. Hu, Y. T. Jiang, X. Y. Wang, J. X. Xu, Q. F. Wang, S. F. Jiang, *Biomass Convers. Biorefin.* **2020**, https://doi.org/10.1007/s13399-020-00976-8.
[64] H. C. Zhang, S. Y. Fu, X. Du, Y. L. Deng, *ChemSusChem* **2021**, *14*, 2268.
[65] J. Lie, Y. C. Lin, J. C. Liu, *Chem. Eng.* **2021**, *167*, 108507.
[66] D. P. Gamliel, B. P. Baillie, E. Augustine, J. Hall, G. M. Bollas, J. A. Valla, *Microporous Mesoporous Mater.* **2018**, *261*, 18.
[67] C. Y. Tu, J. W. Chen, W. L. Li, H. Y. Wang, K. X. Deng, V. A. Vinokurov, W. Huang, *Sustainable Energy Fuels* **2019**, *3*, 3462.
[68] D. P. Gamliel, S. Karakalos, J. A. Valla, *Appl. Catal., A* **2018**, *559*, 20.